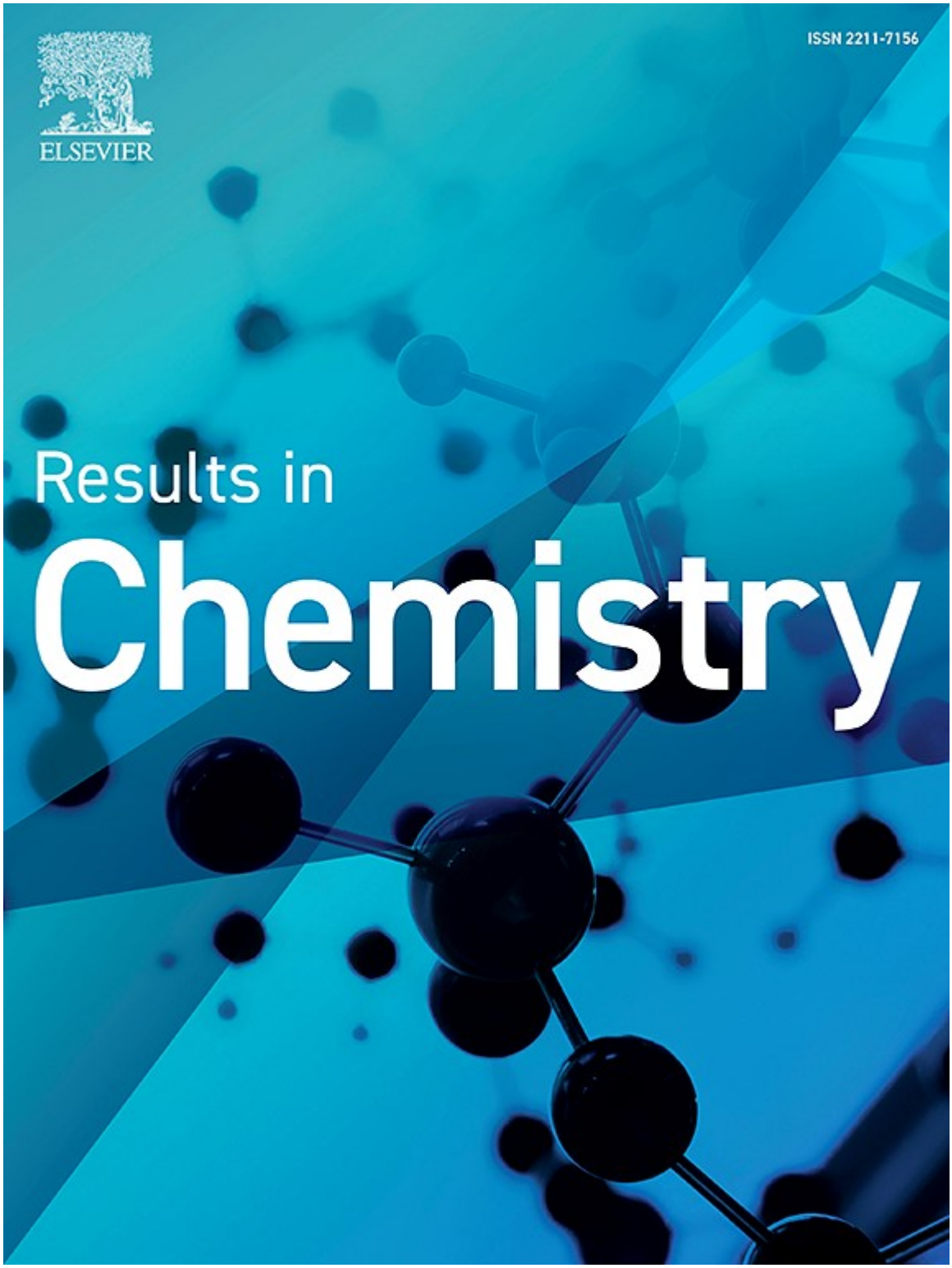
ISSN 2211-7156
ELSEVIER
Results in
Chemistry

Actions for selected articles
Select all / Deselect all

Download PDFs

Export citations

Show all article previews

Contents

Research article • Open access

Synthesis of Zinc(II)-natural zeolite mordenite type as a drug carrier for ibuprofen: Drug release kinetic modeling and cytotoxicity study

Yantus A.B. Neolaka, Yosep Lawa, Magdarita Riwu, Handoko Darmokoesoemo, ... Heri Septya Kusuma
Article 100578

Download PDF Article preview

Research article • Open access

Ultrasound-assisted synthesis, spectral and analytical analysis of g-C_3N_4/CeO_2 composites towards catalytic reduction of nitroaromatic compounds & selective fluorescence detection of Hg^{2+}

D. Venkatesh, G. Deepthi, K. Girija Mangatayaru, M. Noorjahan
Article 100598

Download PDF Article preview

Research article • Open access

Facile synthesis and characterization of noble metals decorated g-C_3N_4 (g-C_3N_4/Pt and g-C_3N_4/Pd) nanocomposites for efficient photocatalytic production of Schiff bases

G. Balraj, Raju Gurrapu, Ambala Anil Kumar, V. Sumalatha, Dasari Ayodhya
Article 100597

Download PDF Article preview

Polymer Chemistry and materials science

Research article • Open access

Editorial board

Editors

Associate Editor

Lorena Betancor, PhD

Universidad ORT Uruguay, Department of Biotechnology, Montevideo, Uruguay

Biocatalysis, Enzyme technology, Bioconversions, Nanobiotechnology, Nanoparticles

View full biography

Scientific Editors

Joyanta Choudhury, PhD

Indian Institute of Science Education and Research Bhopal, Bhopal, India

N-heterocyclic carbene (NHC), CO2 hydrogenation/reduction, C-H activation, Water-soluble catalysts, Heterogenized molecular catalysts

View full biography

Associate Scientific Editors

Thorfinnur Gunnlaugsson, PhD

Trinity College Dublin School of Chemistry, Dublin, Ireland

Supramolecular organic and inorganic chemistry, bio and medicinal chemistry

View full biography

Advisory Board

Alvin Holder, PhD, FRSC, CChem

Old Dominion University Department of Chemistry & Biochemistry, Norfolk, United States of America

Inorganic chemistry, Bioinorganic, Transition metal chemistry, and inorganic reaction mechanisms

View full biography

Jean-Philip Piquemal, PhD

Sorbonne University, Department of Chemistry, Paris, France

Quantum Chemistry and drug design, theoretical chemistry

View full biography

Mark Symes, PhD

University of Glasgow School of Chemistry, Glasgow, United Kingdom

Electrochemistry, Electrocatalysis, Energy conversion, Electrochemical engineering, Electrolysis,

View full biography

Yi-lun Ying, PhD

Nanjing University, Nanjing, China

Dynamic Bioanalysis at the Single Molecule Resolution; Electrochemical Big Data Analysis, Electrical-Optical Confinment; Nanopores.

View full biography

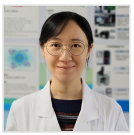

Yuanfeng Li, PhD

The First Affiliated Hospital of Wenzhou Medical University, Wenzhou, China

Polymer chemistry, Nanomaterials, Colloids, Biomaterials, Functional hydrogels, Responsive materials, Controlled release, Biointerfaces

Chaosheng Luo, PhD

Elsevier

Organic chemistry, synthetic methodology, asymmetric organocatalysis and chemical biology

Marta Meazza, PhD

Elsevier Ltd.

Asymmetric Synthesis, Synergistic Catalysis, Organocatalysis, Photocatalysis, Synthesis of Heterocycles

Email this editor

Jessica Pancholi, PhD

Elsevier B.V.

Bioorganic chemistry, 'Click' Chemistry, Medicinal Chemistry, Organic Synthesis/Methodology, Supramolecular Chemistry

Email this editor

Paridhi Saxena, PhD

Elsevier

Organic Synthesis/Methodology, Transition Metal Catalysis, Asymmetric Organocatalysis, Natural Products and Drug design

Email this editor

Vikas Shingade, PhD

Elsevier B.V.

Synthetic chemistry, Molecular spectroscopy, Photochemistry and Photophysics, Medicinal chemistry, Supramolecular chemistry

Email this editor

BUKTI SCOPUS

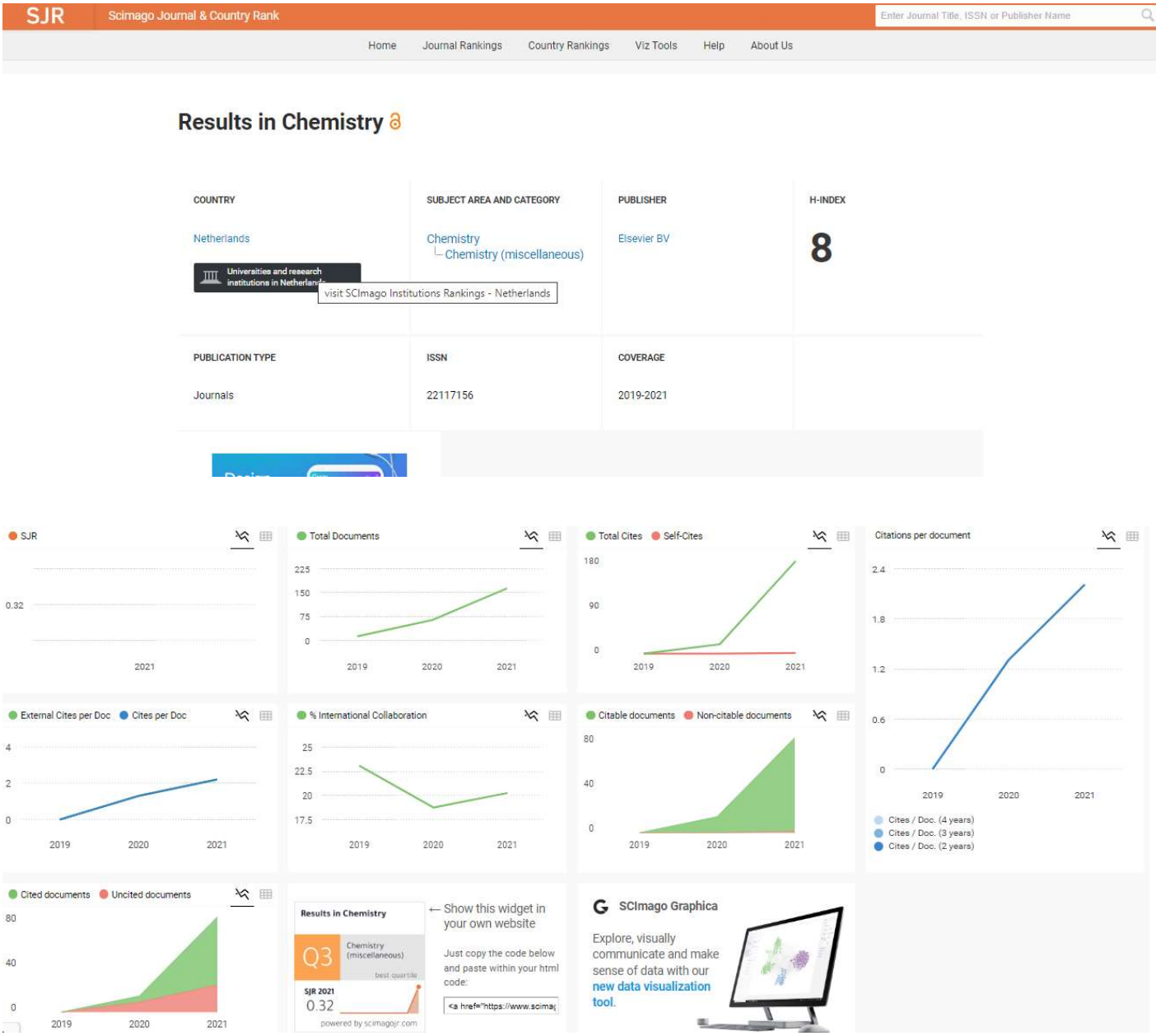

Results in Chemistry 4 (2022) 100578

Contents lists available at ScienceDirect

Results in Chemistry

journal homepage: www.sciencedirect.com/journal/results-in-chemistry

Synthesis of Zinc(II)-natural zeolite mordenite type as a drug carrier for ibuprofen: Drug release kinetic modeling and cytotoxicity study

Yantus A.B. Neolaka [a,*], Yosep Lawa [a], Magdarita Riwu [b], Handoko Darmokoesoemo [c,*], Harsasi Setyawati [c], Johnson Naat [a], Bernadeta Ayu Widyaningrum [d], Uyiosa Osagie Aigbe [e], Kingsley Eghonghon Ukhurebor [f], Robert Birundu Onyancha [g], Heri Septya Kusuma [h,*]

[a] Department of Chemical Education, Faculty of Education and Teachers Training, University of Nusa Cendana, Kupang Nusa Tenggara Timur 85001, Indonesia
[b] Medical School, University of Nusa Cendana, Kupang Nusa Tenggara Timur 85001, Indonesia
[c] Department of Chemistry, Faculty of Science and Technology, Airlangga University, Mulyorejo, Surabaya 60115, Indonesia
[d] Research Center for Biomaterials, National Research and Innovation Agency (BRIN), Jalan Raya Bogor Km 46, Cibinong, West Java 16911, Indonesia
[e] Department of Mathematics and Physics, Faculty of Applied Sciences, Cape Peninsula University of Technology, 1906 Cape Town, South Africa
[f] Department of Physics, Faculty of Science, Edo State University Uzairue, P.M.B. 04, Auchi 312101, Edo State, Nigeria
[g] Department of Physics and Space Science, School of Physical Sciences and Technology, Technical University of Kenya, P.O. Box 52428–, 00200 Nairobi, Kenya
[h] Department of Chemical Engineering, Faculty of Industrial Technology, Universitas Pembangunan Nasional "Veteran" Yogyakarta, Indonesia

ARTICLE INFO

Keywords:
Ibuprofen
Drug Carrier
Mordenite
Drug Safety
Zn(II)

ABSTRACT

Zn(II)-ZMT material development based on natural zeolite mordenite type (ZMT) as a drug carrier for ibuprofen has been explored and assessed. The ion exchange method was carried out to prepare Zn(II)-ZMT material. XRD, FTIR, and FESEM-EDS were used to characterize the physico-chemical characteristics of all materials. The performance of Zn(II)-ZMT as a drug delivery agent for ibuprofen was also evaluated using drug loading-release, zeta potential measurement, and cytotoxicity testing. Six kinetic models (including the zero-order, first-order, Peppas-Sahlin, Higuchi, Hixson-Crowell, and Korsmeyer-Peppas models) were utilized to simulate the drug release process. Meanwhile, a microtetrazolium (MTT) assay was used to analyze the material's cytotoxicity. The Zn(II)-ZMT material has a drug loading content (DLC) of 90.37 % and an efficiency entrapment content (EEC) of 54.22 %, according to drug loading. The drug releases kinetic modeling of Ibuprofen from Zn(II)-ZMT followed the Hixson-Crowell model. This material exhibits good biocompatibility based on a cytotoxicity test using the MTT assay. Ibu@Zn(II)-ZMT has a zeta potential of − 61.55 mV ± 0.1 mV. These findings suggest that the material in the dispersion system has a high degree of stability, indicating that it will not flocculate or coagulate in the body. Furthermore, Zn(II)-ZMT is an inorganic substance that has the potential to be employed as a medication delivery material in the future.

Introduction

Cancer is a disease in which cells lose control of their development and cause aberrant cell proliferation in certain body areas. This abnormal cell development can harm other bodily tissues near cancer through blood veins and lymph vessels. It can move to other body parts distant from its origin (metastasis). The spread of cancer cells to healthy tissues in different body organs might harm them, impairing their ability to function [7]. Treating cancer in the body as soon as possible is critical to prevent aberrant cells from multiplying. Cancer mortality remains high despite advances in understanding cancer's molecular basis, detection, and therapy. Surgery, radiation treatment, chemotherapy, hormone therapy, and immunotherapy have solved this condition [4].

Cancer drugs are usually packaged in a concave shape so that drugs often leak before reaching the cancer target and cause cancer therapy to be not optimal [17]. As a result, cancer therapy necessitates using a carrier material that can regulate medication release, often known as a drug delivery system. A medication delivery system distributes pharmaceuticals directly to target tissues to produce a therapeutic impact without affecting other tissues [29]. Today, drug delivery

* Corresponding authors.
E-mail addresses: yantusneolakaunc@gmail.com (Y.A.B. Neolaka), handoko.darmokoesoemo@gmail.com (H. Darmokoesoemo), heriseptyakusuma@gmail.com (H.S. Kusuma).

https://doi.org/10.1016/j.rechem.2022.100578
Received 16 August 2022; Accepted 13 October 2022
Available online 14 October 2022

nanotechnology has developed with more efficient and specific results. One of these developments is porous inorganic materials in medicinal substances or compounds. Researchers have succeeded in synthesizing porous inorganic drug delivery materials in recent years. One of them is the synthesis of mesoporous silica SBA-15. This material was synthesized using a triblock copolymer mold, Pluronic P123, and tetraethyl orthosilicate (TEOS) as a source of silica [47]. Inorganic materials have water-insoluble qualities, excellent physico-chemical stability, and are leak-proof, medication release can be precisely regulated by using them. Mesoporous silica (MSN) nanoparticles, carbon nanomaterials, and gold nanoparticles are inorganic materials with physicochemical stability for drug delivery agents [17]. However, modifying inorganic nanomaterials is quite tricky, and expensive reagents for synthesis will be considered for using these materials in the future. Naturally porous inorganic materials can be used as an alternative to solve this problem. One example is the use of natural zeolite.

A three-dimensional inorganic crystalline substance made of silicon, aluminum, and oxygen is called zeolite [2]. Zeolites have been widely used in catalysis, ion exchange, adsorption, and separation applications. Recently, it has been known that zeolites have potential in medical applications as a matrix for developing anti-cancer drug molecules [14]. The use of zeolites as carriers of anti-cancer compounds has been reported by Vilaça et al. [46], using 5-fluorouracil as the model drug. Concurrent administration of zeolite and medicine does not eliminate the drug's pharmacological effect. The advantages of zeolite as a drug delivery agent are reducing toxicity, increasing drug efficacy, allowing the drug to be released in a controlled manner into the cancer area, and preventing drug degradation [46]. Natural zeolites have a unique nano-sized pore structure and large surface area. Small pore size can confine drug molecules causing interactions between drug molecules and the pore walls. The structure and mineral content of zeolites vary depending on the formation process. The zeolite used in this study is a natural zeolite-type mordenite obtained from Ende Flores. This natural zeolite consists of quartz and 50 % mordenite [31].

Previously, we have reported preparing natural zeolite mordenite type (Cu(II)-Mor) as a drug carrier for ibuprofen and meloxicam. The results show that this material has a good toxicity value but has low biocompatibility [30]. Therefore, this paper will report another part of our research to improve the biocompatibility of the drug delivery agent we developed based on ZMT from Ende Flores, Indonesia. Modification of ZMT as a drug delivery agent was carried out using Zn(II) as a coordinating cation. The Zn(II) ion was chosen because, in this case, the prepared composite is more homogeneous, uniform, stable and safe for the human body. Zn(II) is also a cofactor of several enzymes and is essential in regulating how neurons can communicate with each other [23].

Evaluating Zn(II)-ZMT as a drug delivery agent and loading and releasing Ibuprofen Zn(II)-ZMT were conducted. Ibuprofen was chosen as a drug model because ibuprofen is reported to have anti-cancer activity, particularly for breast and lung cancer [11,16]. Ibuprofen is a well-known non-steroidal anti-inflammatory medicine (NSAID) used to treat inflammatory rheumatoid arthritis and lessen severe pain [35]. Ibuprofen is synergistic when used with anti-cancer drugs to reduce colon tumor size [21]. The physico-chemical characterization of Zn(II)-ZMT and Ibu@Zn(II)-ZMT materials was led by using X-ray Diffraction (XRD) and Fourier Transform InfraRed (FTIR) and Field Emission Scanning Electron Microscopy with Energy Dispersive X-ray Spectroscopy (FESEM-EDX). We will also report drug release kinetics modeling using six kinetic models: zero-order, first-order, Peppas-Sahlin, Higuchi, Hixson-Crowell, and Korsmeyer-Peppas. Appropriate kinetic models will help determine designs in drug delivery applications. Furthermore, the determination of the zeta potential of the Ibu@Zn(II)-ZMT material and the cytotoxicity test of the Zn(II)-ZMT and Ibu@Zn(II)-ZMT materials using the microtetrazolium (MTT) assay will also be reported too.

Materials and methods

Reagents and materials

The Tropical Disease Diagnostic Center Airlangga University in Surabaya, Indonesia, provided the African green monkey kidney cells (Vero). In our laboratory, reverse osmosis (RO) water and activated natural zeolite from Ende Flores, Indonesia, were created. 99.0 % sodium chloride (NaCl), 99.0 % ZnSO4·.7H2O ReagentPlus®, and pH 4, pH 7, and pH 9 buffers. MTT Reagent (3-(4,5-dimethylthiazole-2-yl)-2,5-diphenyltetrazolium bromide), Minimum Essential Medium Eagle (MEM), Dimethyl sulfoxide (DMSO), Phosphate-Buffered Saline (PBS), Trypsin-EDTA solution, Fetal Bovine Serum (FBS), and Trypan Blue are some of the other ingredients in DMEM (Dulbecco's The P.T. Merck Chemicals and Life Sciences PP Plaza 4th floor, Jalan TB. Simatupang 57 Jakarta 13,760 was used for the acquisition of all chemicals.

Zn(II)-ZMT material preparation

The method approach by Khatamian et al., [23] 11 was used to prepare the Zn(II)-ZMT material. ZMT (0.5 g) was agitated for 24 h while suspended in a 5 mL, 3 M NaCl solution. The finished powder was then separated and thoroughly cleaned using demineralized water in a centrifuge at 2000 rpm before being dried at 60 °C. The ZMT powder was mixed with a 25 mL, 1 M solution of $ZnSO_4{\cdot}7H_2O$ for 24 h, separated, and repeatedly rinsed with demineralized water in a centrifuge at 2000 rpm, and finally dried at 60 °C.

Drug carrier characterization

The instrumentation such as X-ray diffraction (Shimadzu XRD 7000, Japan), FESEM-EDS (Thermo Scientific Quatro S), and FTIR (Perkin Elmer, with attenuated total reflectance method at a resolution of 4 cm-1 in the range of 400–4000 cm-1, scan 16 times) was used to characterize The Physico-chemical properties of Zn(II)-ZMT and Ibu@Zn(II)-ZMT materials.

Zeta potential measurement

Zeta potential Horiba SZ-100, dispersant Aquadest, Size range ± 200 mV, was used to research the stability of the drug-carrier material's dispersion. Before measurement, Zn(II)-ZMT and Ibu@Zn(II)-ZMT were crushed in RO water.

Ibuprofen calibration curve

The calibration curve was using ibuprofen (1000 ppm ibuprofen mg/L), a standard solution. It made a series of these standard solutions with concentrations ranging from 2 mg/l to 16 mg/L. Then the solution was measured using UV–vis at a wavelength of 200 nm. In this study, the linear equation used for the ibuprofen calibration curve was $y = 0.0021x + 0.0137$.

Loading ibuprofen on Zn(II)-ZMT

Loading Ibuprofen was carried out using the method by Karavelidis et al., [22] and Sun et al., [44] with significant modifications. A total of 1000 mg of Zn(II)-ZMT was put in several separate containers with a volume of 75 mL, each containing 600 mg of ibuprofen. Then the mixture was stirred at room temperature for 1 to 24 h. After the stirrer process, the sample was filtered and dried at 30 °C for 2 h. Meanwhile, the filtrate was measured using UV–vis at a wavelength of 200 nm. The results of loading ibuprofen on Zn(II)-ZMT (Ibu@Zn(II)-ZMT) were then calculated using the percentage of drug loading content (DLC, %) and entrapment efficiency content (EEC, %) equations are still determined through equations (1) and (2), respectively [22].

$$\text{Drug loading content}\,(\%) = \frac{\text{Weight of drug in Zn(II)} - \text{ZMT}}{\text{Weight of Zn(II)} - \text{ZMT}} \bullet 100 \quad (1)$$

$$\text{Entrapment Efficiency content}\,(\%) = \frac{\text{Weight of drug in Zn(II)} - \text{ZMT}}{\text{Weight of drug fed initially}} \bullet 100 \quad (2)$$

2.7 Drug release ibuprofen from Zn(II)-ZMT

Ibu@Zn(II)-ZMT samples were divided into 50 mL of pH 7 buffer solution, pH 4 acid buffer solution, and pH 9 alkaline buffer solution. Then, the solution was stirred for 24 h. The sample solution was then obtained at regular intervals of 5 mL, and 5 mL of a buffer solution with the same pH was added, keeping the sample volume at 50 mL. A particular wavelength was then measured using UV–vis at 200 nm after 5 mL of the solution had been centrifuged at 1500 rpm for 5 min. The level of ibuprofen in the sample solution does not change after a certain amount of desorption time. Presumably, the medicine has been released.

2.8 Cytotoxicity (MTT assay) material

The Vero cell cytotoxicity test was performed using the MTT method. In this study, ATCC CCL-81-designated Vero cells were utilized. These Vero cells were isolated using the kidney of an African green monkey. Vero cells were first introduced to the DMEM culture medium with a cell density of 5 × 104 cells/mL for the cytotoxicity test. The cells were then put in 96-well plates, where they were cultured for 24 h at 37 °C with 5 % CO2 content.

The material was discarded, and Phosphate Buffer Saline was cleaned after 24 h (PBS). Zn(II)-ZMT or Ibu@Zn(II)-ZMT is the sample at that point. In this investigation, the concentrations of Zn(II)-ZMT and Ibu@Zn(II)-ZMT were adjusted to 200 μg/mL, 100 μg/mL, 50.25 μg/mL, 12.5 μg/mL, and 6.25 μg/mL. This step was carried out by triplication. Some wells just had solvent poured into them as a negative control. When orange formazan had developed after 4 h of incubation at 37 °C and 5 % CO2, 10 L of MTT reagent was added. The analysis was then conducted using an ELISA multiplate reader at 595 nm [34]. The calculation of the percentage of living cells was completed using Equation (3).

$$\text{Live Cells}\,(\%) = \frac{\text{The absorbance of treatment} - \text{Absorbance of control media)}}{\text{The absorbance of control of cells} - \text{Absorbance of control of media}} \bullet 100 \quad (3)$$

Results and discussion

Synthesis of Zn(II)-ZMT

Mordenite-type natural zeolite (ZMT) was modified to form a Zn(II)-ZMT material. The ZMT sample was first suspended in a NaCl solution. NaCl is used to maximize the ion exchange power and adsorb of ZMT. Research conducted by Cheng et al., [6] showed that the zeolite, after modification with NaCl, had a larger pore size to increase the adsorption capacity. Furthermore, the ZMT suspended in the NaCl solution is modified with the coordination cation, Zn(II), by adding the ZMT to the $ZnSO_4{\cdot}7H_2O$ solution. The modification with Zn(II) is to stabilize ZMT. ZMT with Zn(II) is modified through ion exchange. Zeolite has a negatively charged part, Al^{3+}, where an Al atom with a valence of 3 must bind four oxygen atoms. This negative charge allows zeolites to bind cations with weak bonds such as Na. Because of this weak bond, Na ions can be exchanged for Zn(II) metal ions.

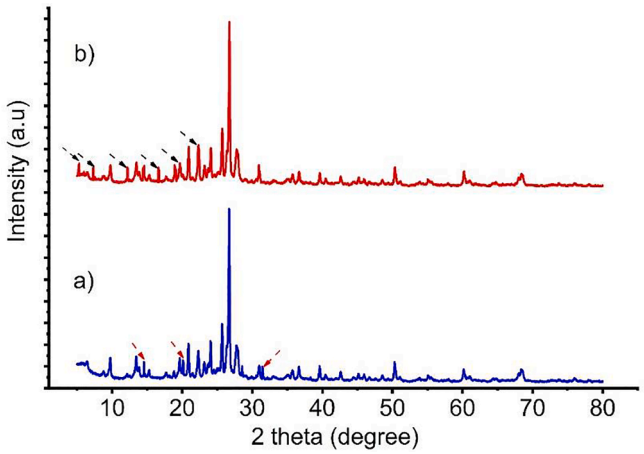

Fig. 1. The diffractogram for: (a) Zn(II)-ZMT and (b) Ibu@Zn@ZMT.

Characterization of Zn(II)-ZMT

XRd

XRD characterization was carried out on Zn(II)-ZMT and Ibu@Zn(II)-ZMT materials to see whether the Zn(II)-ZMT synthesis affected the crystallinity change of ZMT or not. Besides that, to see if there is a change in crystallinity and ibuprofen loading on Zn(II)-ZMT. A typical reflection's high and low intensities will reveal the material's crystallinity [32]. The results of the characterization of Zn(II)-ZMT and Ibu@Zn@ZMT using XRD are presented in Figure 1fig1.

Fig. 1a) is a diffractogram of Zn(II)-ZMT. Fig. 1a), three typical intensities of Zn sulfate appear at 2θ: 14.52°, 20.15°, and 31.51°. These results are related to research by Saha & Podder [39] and Ersan et al., [9]. Fig. 1 a) indicates that the synthesis of Zn(II)-ZMT has been successfully carried out. Fig. 1b) is the Ibu@Zn(II)-ZMT diffractogram. It is known that ibuprofen has a characteristic reflection intensity that will appear in the interplanar direction, which is 14.5°, 7.2°, 5.3°, 4.7°, and 4.0°, with typical peaks at 6.1°, 12.2°, 16.6°, 19.0° and 22.3°. [27]. Based on Fig. 1b), it can be seen that the typical diffractogram at 2θ corresponds to the specific reflection of ibuprofen, namely at 5.34°, 7.33°, 12.09°, 16.63°, 19.68°, and 22.28°. These results indicate that loading ibuprofen on Zn(II)-ZMT was successful.

FTIr

The characterization of drug delivery materials using FTIR is intended to see the presence of new bonds or functional groups in these materials and to determine whether the target drug has been properly loaded on the drug delivery material. [1]. The results of the characterization of Zn(II)-ZMT and Ibu@Zn@ZMT using FTIR are presented in Figure 2fig2.

In Fig. 2 (black color), it can be seen that there is a distinctive peak that appears at a wavenumber of ± 3000 cm^{-1}. The peak at ± 3000 cm^{-1} is related to the hydroxyl group's peak in the water molecule to a lower frequency. The action of Zn(II) interacting with the water

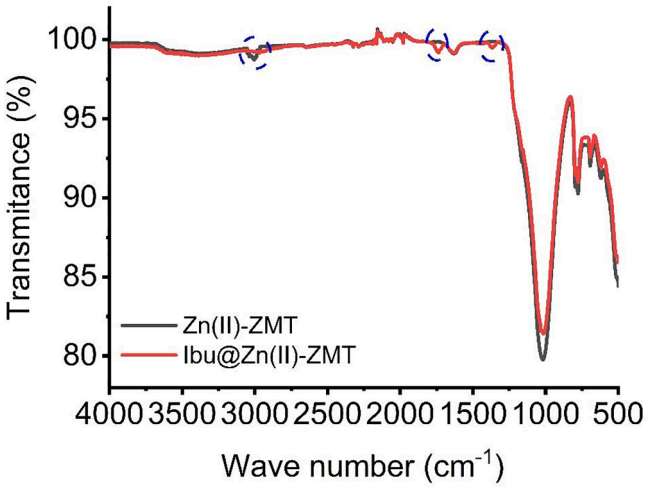

Fig. 2. FTIR Spectra of Zn(II)-ZMT and Ibu@Zn@ZMT.

molecule's O atom causes the decreased water frequency in this peak [12]. The spectra in Fig. 2 (red color) show a characteristic peak at wave number 1731.38 cm^{-1}, a free carboxyl acid group from ibuprofen. The peak visible at wave number 1362.17 cm^{-1} is a carboxylate ion group, which is a typical peak indicating that ibuprofen has been successfully loaded in the ZMT matrix [25].

FESEM-EDx

FESEM is used to see the morphological differences in the drug delivery material before and after loading. The elemental composition before or after loading is also determined using EDS simultaneously. FESEM-EDX characterization for Zn(II)-ZMT and Ibu@Zn(II)-ZMT materials is presented in Fig. 3. ibuprofen (Fig. 3b1). These results indicate that ibuprofen has covered or filled the pores of the Zn(II)-ZMT material. EDX data showed a reduction in the elemental composition of Zn(II) from 2.0 % (Fig. 3. a2) to 1.6 % (Fig. 3. B2) after drug loading. EDX analysis of Zn(II)-ZMT and Ibu@Zn(II)-ZMT clearly showed a reduction in Zn(II) elements after loading with ibuprofen. The decrease in Zn(II), Na+, Si, and Al, along with the increase in C and O atoms after loading ibuprofen, indicates that there is a slight change in the crystal structure of this drug delivery material due to a subtle shift in the stoichiometric equilibrium of the elements in the Zn(II)-ZMT framework. This EDX data

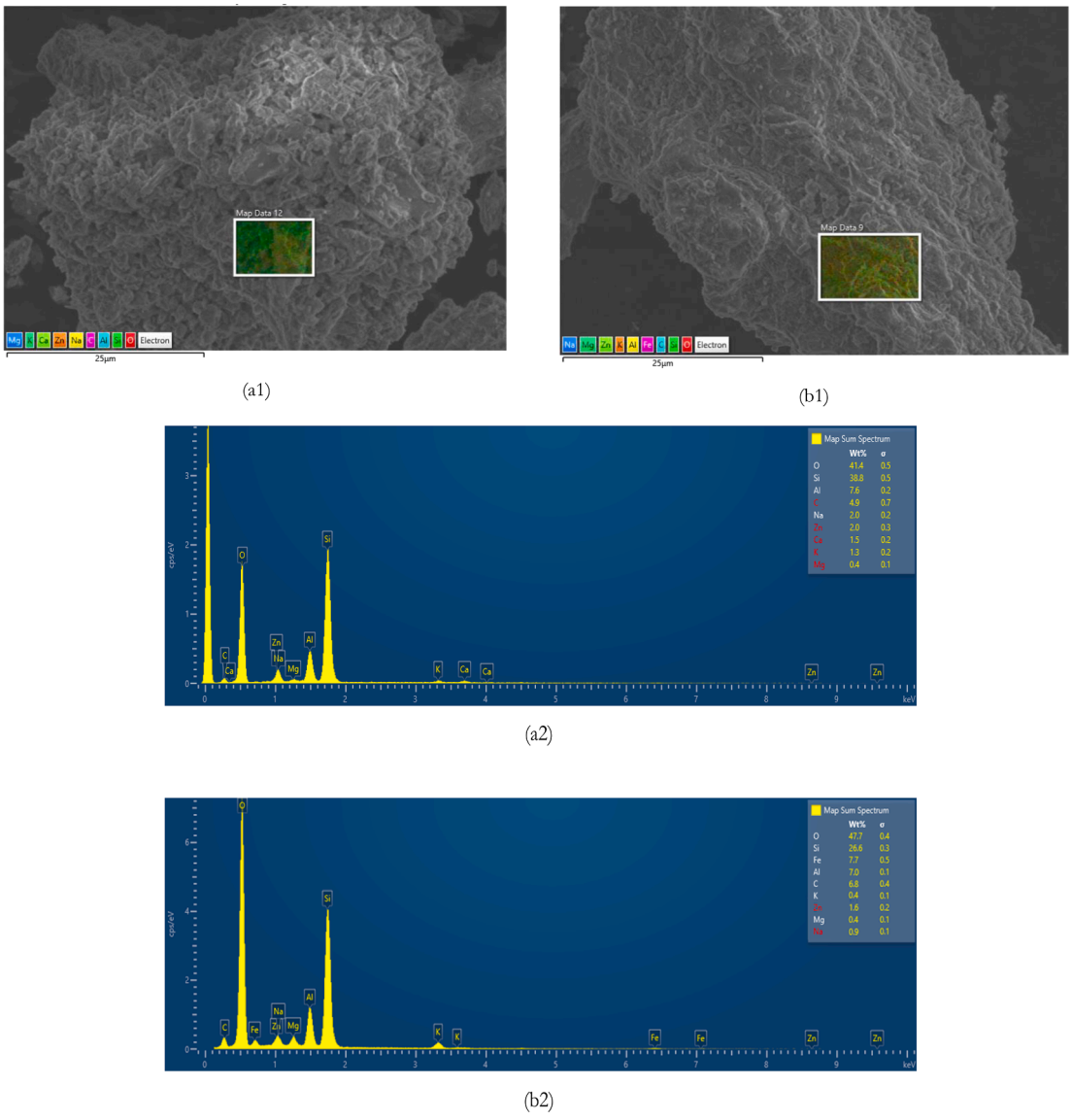

Fig. 3. FESEM-EDS images of: (a1) FESEM of Zn(II)-ZMT; (a2) EDS of Zn(II)-ZMT; (b1) FESEM of Ibu@Zn(II)-ZMT; and (b2) EDS of Ibu@Zn(II)-ZMT.

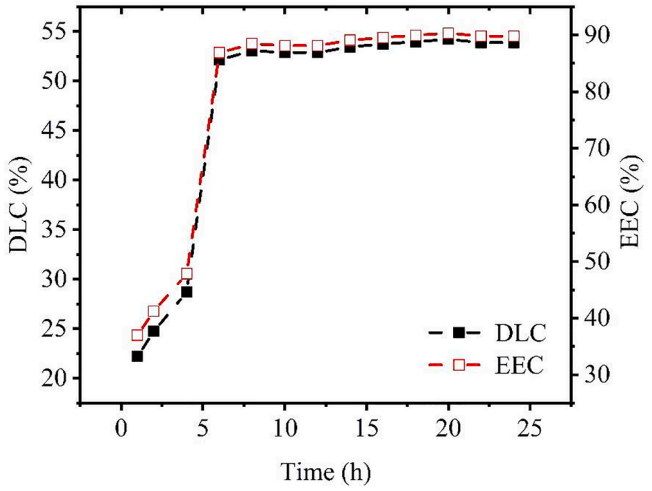

Fig. 4. EEC and DLC values of loading ibuprofen on Zn(II)-ZMT.

can be used to reference that there has been a new bond interaction between the carrier and drug through specific interaction mechanisms. The bond interactions between the carrier and the drug are referred to as non-bonding interactions, van der Waals and coulombic electrostatic interactions.

Investigating drug loading capacity

Fig. 4 shows the drug loading time graph versus DLC (%) or EEC (%). Drug loading was led from 2 to 24 h. It can be noticed that during 2–4 h, ibuprofen's loading on Zn(II)-ZMT varies between 41 and 47 % and then increases again between 80 and 90 % for a loading time of 6 to 24 h (by using equations (1) and (2)). The highest loading occurred at a loading time of 20 h with a DLC value of 90.37 % and an EEC of 54.22 %. These results align with research conducted by Sun et al., [43] and Sun et al., [44]. The effect of loading ibuprofen indicates that Zn(II)-ZMT has the potential to be used as a drug delivery agent.

Drug release kinetic modeling

The dissolution test can determine the drug release profile. Dissolution is when a stable enters a solvent and becomes a solution [5]. The quantitative values obtained from the dissolution test were analyzed to a mathematical model to make it easier to describe the drug release kinetics modeling. In this study, the release of Ibuprofen from Zn(II)-ZMT was observed in various solutions, namely pH 4 (acidic state), which was adjusted to gastric conditions, pH 7 (neutral form), which was converted to physiological needs of the blood and pH 9 (an alkaline state). This pH difference is made to determine the optimum pH. The selected time interval is 60 min for 24 h. The drug release test aimed to determine Zn (II)-ZMT efficiency and effectiveness as a drug delivery agent. Six kinetics models, namely, zero order, first order, Peppas-Sahlin Higuchi, Hixson-Crowell, and Korsmeyer-Peppas models, were used to determine the study drug release mechanism.

Zero-order model

The ideal drug release is to follow a zero-order kinetics model with constant drug release from start to finish. The increase in drug release is directly proportional to time. The drug release data obtained in vitro is plotted as the cumulative amount of drug regardless of the function of time to produce a linear graph [26]. The drug is dissolved according to equation (4).

$$Q_t = Q_0 + K_0 \bullet t \tag{4}$$

where Q_t stands for the drug's quantity at time t, Q_o for its starting concentration in solution, and K_o for its zero-order release constant. Zero-order release kinetics can also describe the dissolution of modified drug dosage forms, such as multiple transdermal systems, osmotic systems, tablet matrixes with low solubility drugs, etc. [13].

First-order model

The exposed surface area of the tablets decreased exponentially with time during the dissolution process, indicating that drug release from most of the slow-release tablets could be explained by first-order kinetics. The first-order equation is obtained from the log percent remaining drug plot as a time function, producing a linear graph [37]. First-order drug release kinetics follow equation (5).

$$\log Q_t = \log Q_0 + \frac{K_1 \bullet t}{2.303} \tag{5}$$

where Q_t stands for the drug's quantity at time t, Q_o is for its starting concentration in solution, and k_1 is the first-order drug release constant.

Peppas-Sahlin model

The Peppas-Sahlin model describes measuring the contribution of diffusion and relaxation of polymers. The release kinetics of the Peppas Sahlin model is shown by equation (6).

$$Q_t = K_1 \bullet t^m + K_2 \bullet t^{2m} \tag{6}$$

where Q_t stands for the drug's quantity at time t, K_1 and K_2 are Peppas-Sahlin constants, and m is the purely Fickian diffusion exponential [36].

Higuchi model

As a diffusion process, the Higuchi model addresses the release of soluble and less soluble medicines in the water contained in a solid matrix. According to this concept, the amount of medicine released and the time root have a linear connection. Due to the more considerable drug diffusion distance, the medication will be delivered slowly the longer the given period. A straight line may be drawn by plotting the roots of time against the cumulative amount of medication dissolution. The Higuchi drug release kinetics model is based on equation (7).

$$Q_t = K_H \bullet \sqrt{t} \tag{7}$$

where Q_t is the drug's quantity at time t and K_H is the Higuchi constant [18].

Hixson-Crowell model

The Hixson-Crowell model depicts the dissolution discharge from a system in which the surface area and diameter of the particles change as a function of time. The Hixson-Crowell model of drug release kinetics follows the equation (8).

$$\sqrt[3]{Q_t} - \sqrt[3]{Q_0} = K_{HC} \bullet t \tag{8}$$

where Q_t stands for the drug's quantity at time t, Q_o is for its starting concentration in solution, and K_{HC} is the Hixson-Crowell constant [19].

Korsmeyer-Peppas model

The Korsmeyer-Peppas model derives the relationship describing drug release from the polymer system. The Korsmeyer-Peppas model of drug release kinetics follows the equation (9).

$$\log \frac{Q_t}{Q_0} = \log K + n \bullet \log t \tag{9}$$

where Q_t stands for the drug's quantity at time t, K is the kinetic constant, and Q_o is the quantity of medication released at infinite time t. n is the diffusion exponent indicating the drug transport mechanism through the polymer. The kinetics of the Korsmeyer-Peppas model depends on the value of n, where the value of $n < 0.89$ for drug release is referred to as the super case II transport mechanism. Plots depicting the cumulative percentage of drug release against the log of time display data from in vitro drug release investigations [24,26]. The calculated values of n ($n > 0.5$) exponential form Korsmeyer Peppas equation in different pH media, also indicating that the release mechanism follows the non-Fickian mechanism [3;28].

Based on six kinetics modeling for drug release, the release of Ibuprofen from Zn(II)-ZMT is plotted by time-release vs percentage of dissolution. Fig. 5 shows graphs of different modeling drug release kinetics of Zn(II)-ZMT at various pH. Table 1 shows the findings of modeling drug release of Zn(II)-ZMT at different pH levels.

Based on Fig. 6 and Table 1, the maximum release of Ibuprofen from Zn(II)-ZMT occurred at 1080 min and pH 7 with a current dissolution of 96.747 %. This release amount was higher at pH 7 (96 %), indicating that the Ibu@Zn(II)-ZMT possessed a pH-triggered mechanism for regulating release [41]. At pH 7, the total surface charge of the zeolite became negative, which resulted in a repulsive force between the negative charge of the zeolite and the negative charge of ibuprofen. This forces ibuprofen to separate from Zn(II)-ZMT. Meanwhile, at pH 4 and 9, the active sites of the zeolite are protonated, causing these sites to be neutrally charged and causing ibuprofen to remain trapped in the zeolite framework [8]. At pH 7, there is a conformational shift on the surface of the zeolite, which weakens the hydrogen bond and increases the electrostatic force on the zeolite, resulting in the maximum release. pH affects several structural bonds on the surface of the zeolite. Then these changes cause changes in density so that the bonds that bind or hold ions in the zeolite pores are broken, and the drug can be released [48].

Based on statistical calculations using DDsolver, the release of Ibuprofen from Zn(II)-ZMT followed the Hixson-Crowell model. The Hixson-Crowell model was chosen because the highest adjusted R^2 value was 0.9668. This result is supported by the low values of the sum of squares (SS) and the Akaike information criterion (AIC) [45]. According to Hixson-Crowell, the dissolving rate is determined by the cube root of the particle weight, and the particle radius is not constant. The Hixson-Crowell principle depicts the dissolution rate as a function of time for a decrease in the surface area of a solid, with the system release observed when the surface area and particle diameter vary [38]. These findings suggest that changes in the surface area and particle diameter of the particles or tablets cause ibuprofen to be released from Zn(II)-ZMT material [33].

Zeta potential of Ibu@Zn(II)-ZMT

The zeta potential is commonly employed to determine a particle's surface charge and the materials' stability because changes in these features would directly impact the biological activity of specific nanoparticles [42]. The pharmacokinetics of nanosystem characteristics in the body can be affected by zeta potential [20]. Zeta potential of Ibu@Zn(II)-ZMT is shown in Fig. 6.

Fig. 6 reveals that the zeta potential of Ibu@Zn(II)-ZMT is − 61.55 mV ± 0.1 mV, indicating a significant zeta potential value (negative value). These findings suggest that this material will be moderately stable in a dispersion system, where there will be a strong repulsion

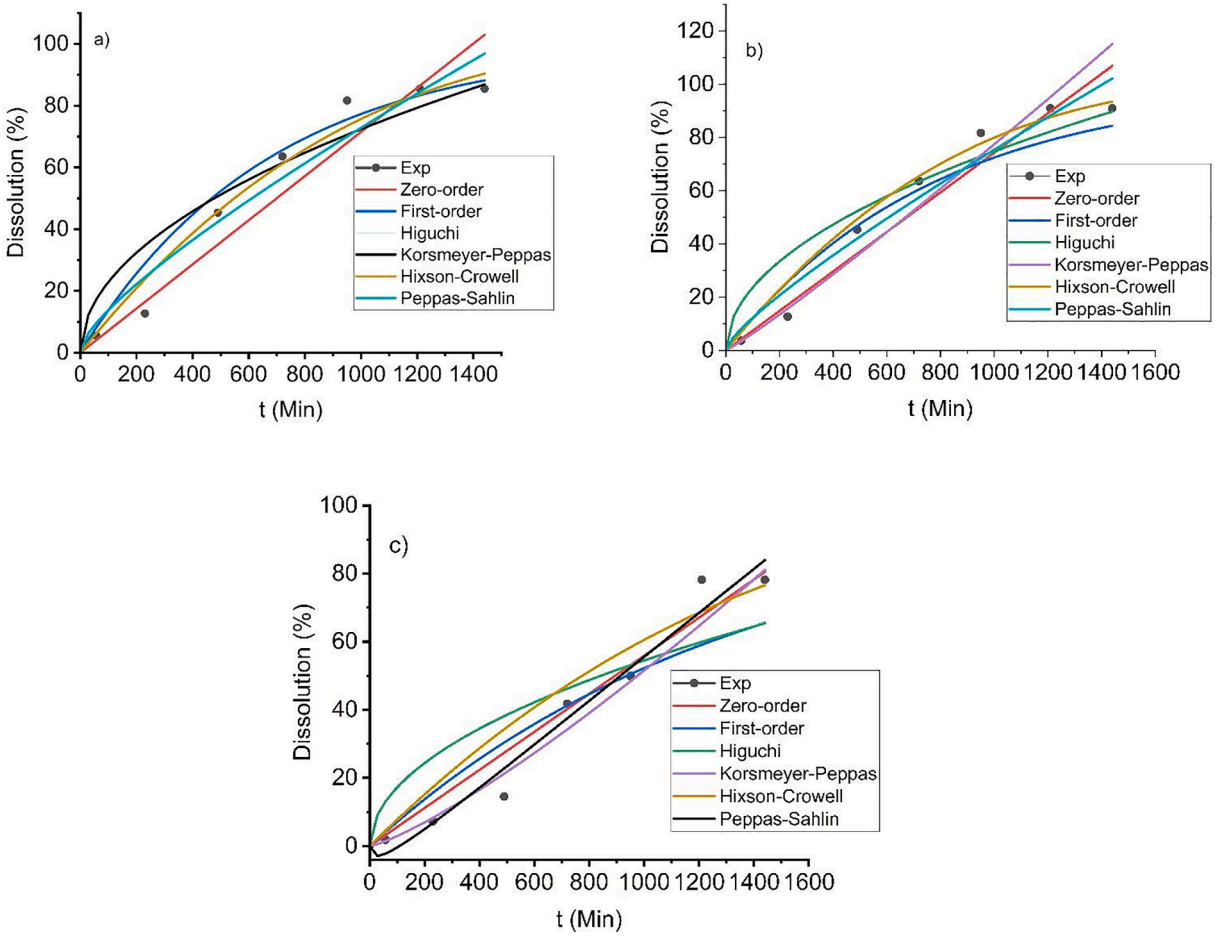

Fig. 5. Ibuprofen release from Zn(II)-ZMT: (a) pH 4; (b) pH 7; and (c) pH 9.

Table 1
Calculation of statistical indicators for the release of Ibuprofen from Zn(II)-ZMT using DDsolver at various pH.

Indicator	Zero Order	First Order	Higuchi	Hixson– Crowell	Korsmeyer-Peppas	Peppas-Sahlin
Release Ibuprofen from Zn(II)-ZMT at pH 4						
R^2 adjusted	0.8902	0.9445	0.8780	0.9657	0.9008	0.9293
SS	765.0440	386.6163	850.3148	238.9168	691.3758	492.9883
AIC	48.4795	43.7020	49.2192	40.3328	49.7708	49.4034
Release Ibuprofen from Zn(II)-ZMT at pH 7						
R^2 adjusted	0.9248	9.9335	0.8754	0.9668	0.8901	0.9474
SS	592.6000	524.4092	981.8476	262.0165	866.0609	414.3767
AIC	46.6916	45.8359	50.2261	40.9789	51.3477	48.1874
Release Ibuprofen from Zn(II)-ZMT at pH 9						
R^2 adjusted	0.9456	0.8609	0.7434	0.8877	0.9532	0.9630
SS	336.6978	860.4284	1587.8093	694.7794	289.2504	229.1593
AIC	42.7343	49.3020	53.5908	47.8052	43.6710	44.0409

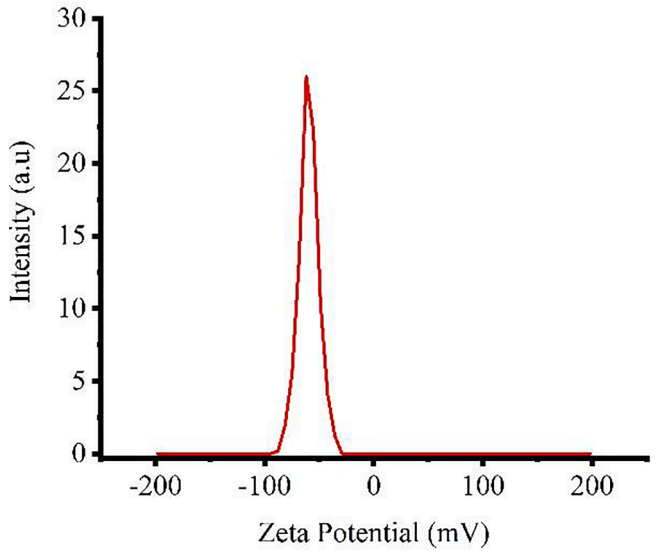

Fig. 6. Zeta potential graph of Ibu@Zn(II)-ZMT.

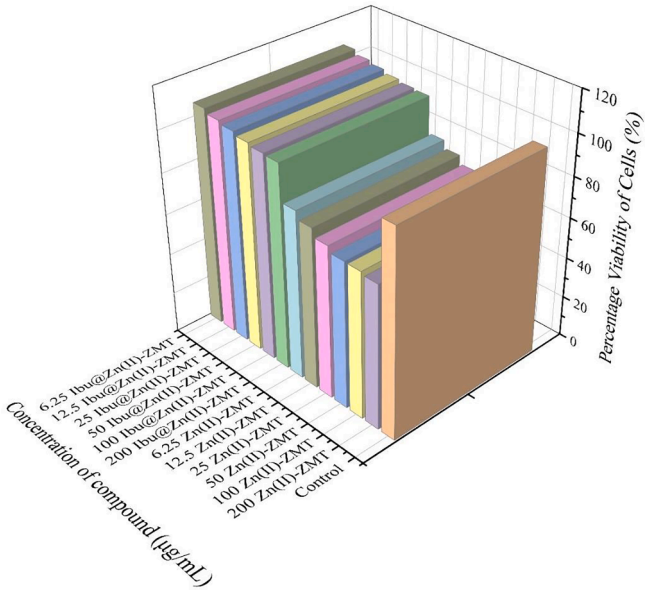

Fig. 7. Cytotoxic effect of Ibu@Zn(II)-ZMT on Vero cell by using the MTT assay.

between the charges in the material to avoid flocculation and coagulation of the particles in the system [30]. Lower Zeta potential levels indicate an increased propensity for aggregation [40]. The Ibu@Zn(II)-ZMT material's zeta potential was as expected, suggesting that it can be employed as a drug delivery system for cancer cell therapy. The likelihood of hazardous side effects from these heavy metals is decreased because these drug particles, which function as anti-cancer drug delivery materials, will not interact strongly with normal cells on the surface of cancer.

Cytotoxicity of drug carrier materials

A substance with a cell viability rating greater than 80 % is said to have minimal cytotoxicity [10,30]. It is known that Mordenite has the potential as a drug delivery system [15]. The diagram of the cytotoxicity test results using the MTT assay is presented in Fig. 7.

Fig. 7 illustrates that when the concentration of Zn(II)-ZMT is less than 6.25 g/mL, it has low toxicity. Vero cell survival values for Zn(II)-ZMT was more than 90 % in all these concentrations, indicating that Zn (II)-ZMT was biocompatible. Observations were also made of Zn(II)-ZMT that had been loaded with the analgesic medication ibuprofen (Ibu@Zn(II)-ZMT) in this cytotoxicity assay. Fig. 7 shows that Ibu@Zn (II)-ZMT has more significant Vero cell viability than 90 %. Because of its outstanding biocompatibility, Zn(II)-ZMT has the potential to be used as an analgesic drug carrier, according to the findings.

Conclusion

The production of a drug delivery agent (Zn(II)-ZMT) for ibuprofen based on natural zeolite mordenite type modified by Zn(II) has been completed effectively. XRD, FTIR, and FESEM-EDS were used to characterize drug delivery materials before and after loading ibuprofen. Six models are used in drug loading investigations and drug release kinetic modeling: zero-order, first-order, Higuchi, Hixson-Crowell, Korsmeyer-Peppas, and Peppas-Sahlin. Researchers measured the material's zeta potential and cytotoxicity to assess the safety of utilizing Zn(II)-ZMT as a medication delivery agent. This material's ibuprofen loading data (Ibu@Zn(II)-ZMT) has a DLC value of 90.37 % and an EEC value of 54.22 %. The Hixson-Crowell model with an R^2 value of 0.9668 describes this substance's kinetics of ibuprofen release. A significant zeta potential value (negative value) of $-$ 61.55 mV $\pm$ 0.1 mV indicates that the material is very stable in the dispersion system. Furthermore, the zeta potential value results show that drug release from the Zn(II)-ZMT material happens to be due to changes in the surface area and particle diameter of the particles or tablets. The MTT technique of cytotoxicity testing revealed that this substance is not harmful and may be employed as a medication delivery agent.

CRediT authorship contribution statement

Yantus A.B. Neolaka: Conceptualization, Methodology, Investigation, Writing – original draft. **Yosep Lawa:** Investigation, Resources, Visualization. **Magdarita Riwu:** Methodology, Validation, Formal analysis, Writing – review & editing. **Handoko Darmokoesoemo:** Methodology, Formal analysis. **Harsasi Setyawati:** Investigation, Resources, Visualization. **Johnson Naat:** Investigation, Resources, Visualization. **Bernadeta Ayu Widyaningrum:** Investigation, Resources, Writing – original draft, Visualization. **Uyiosa Osagie Aigbe:** Methodology, Formal analysis. **Kingsley Eghonghon Ukhurebor:** Methodology, Formal analysis. **Robert Birundu Onyancha:** Methodology, Formal analysis. **Heri Septya Kusuma:** Validation, Writing – review & editing, Supervision.

Declaration of Competing Interest

The authors declare that they have no known competing financial interests or personal relationships that could have appeared to influence the work reported in this paper.

Data availability

No data was used for the research described in the article.

Acknowledgments

The Ministry of Education, Culture, Research and Technology of the Republic of Indonesia is gratefully acknowledged for the Basic Research Grant No. B/1176/E3/RA.00/2020 was awarded to the first author. For their contributions to this research, the first author additionally acknowledges Maria F. Bui, Esmiralda C. Wila, Mutiah A. Fahirah, and Titah Aldila Budiastanti.

References

[1] A.A. Adu, Y.A.B. Neolaka, A.A.P. Riwu, M. Iqbal, H. Darmokoesoemo, H. S. Kusuma, Synthesis, characterization and evaluation of swelling ratio on magnetic p53-poly (MAA-co-EGDMA)@ GO-Fe3O4 (MIP@ GO-Fe3O4)-based p53 protein and graphene oxide from kusambi wood (Schleichera oleosa), J. Mater. Res. Technol. 9 (5) (2020) 11060–11068, https://doi.org/10.1016/j.jmrt.2020.08.003.

[2] R. Amorim, N. Vilaça, O. Martinho, R.M. Reis, M. Sardo, J. Rocha, A.M. Fonseca, F. Baltazar, I.C. Neves, Zeolite structures loading with an anti-cancer compound as drug delivery systems, J. Phys. Chem. C 116 (48) (2012) 25642–25650, https://doi.org/10.1021/jp3093868.

[3] M.M. Ayad, N.A. Salahuddin, A.A. El-nasr, N.L. Torad, Amine-functionalized mesoporous silica KIT-6 as a controlled release drug delivery carrier, Microporous Mesoporous Mater. 229 (2016) 166–177, https://doi.org/10.1016/j.micromeso.2016.04.029.

[4] R. Baskar, K.A. Lee, R. Yeo, K.-W. Yeoh, Cancer and radiation therapy: current advances and future directions, Int. J. Medical Sci. 9 (3) (2012) 193–199, https://doi.org/10.7150/ijms.3635.

[5] N. Blagden, M. de Matas, P.T. Gavan, P. York, Crystal engineering of active pharmaceutical ingredients to improve solubility and dissolution rates, Adv. Drug Deliv. Rev. 59 (7) (2007) 617–630, https://doi.org/10.1016/j.addr.2007.05.011.

[6] Q. Cheng, H. Li, Y. Xu, S. Chen, Y. Liao, F. Deng, J. Li, Study on the adsorption of nitrogen and phosphorus from biogas slurry by NaCl-modified zeolite, PLoS ONE 12 (5) (2017) 1–12, https://doi.org/10.1371/journal.pone.0176109.

[7] M. Egeblad, E.S. Nakasone, Z. Werb, Tumors as organs: complex tissues that interface with the entire organism, Dev. Cell 18 (6) (2010) 884–901, https://doi.org/10.1016/j.devcel.2010.05.012.

[8] Z.S. Eren, S. Tunçer, G. Gezer, L.T. Yildirim, S. Banerjee, A. Yilmaz, Improved solubility of celecoxib by inclusion in SBA-15 mesoporous silica: Drug loading in different solvents and release, Microporous Mesoporous Mater. 235 (2016) 211–223, https://doi.org/10.1016/j.micromeso.2016.08.014.

[9] A.C. Ersan, A.S. Kipcak, M.Y. Ozen, N. Tugrul, An accelerated and effective synthesis of zinc borate from zinc sulfate using sonochemistry, Main Group Met. Chem. 43 (1) (2020) 7–14, https://doi.org/10.1515/mgmc-2020-0002.

[10] M.Z. Fahmi, A. Haris, A.J. Permana, D.L.N. Wibowo, B. Purwanto, Y.L. Nikmah, A. Idris, Bamboo leaf-based carbon dots for efficient tumor imaging and therapy, RSC Adv. 8 (67) (2018) 38376–38383, https://doi.org/10.1039/C8RA07944G.

[11] S.I. Farooqi, N. Arshad, P.A. Channar, F. Perveen, A. Saeed, F.A. Larik, A. Javed, M. Yamin, New aryl Schiff bases of thiadiazole derivative of ibuprofen as DNA binders and potential anti-cancer drug candidates, J. Biomol. Struct. Dyn. 39 (10) (2021) 3548–3564, https://doi.org/10.1080/07391102.2020.1766569.

[12] Z. Fereshteh, M.R. Loghman-Estarki, R. Shoja Razavi, M. Taheran, Template synthesis of zinc oxide nanoparticles entrapped in the zeolite y matrix and applying them for thermal control paint, Mater. Sci. Semicond. Process. 16 (2) (2013) 547–553, https://doi.org/10.1016/j.mssp.2012.08.005.

[13] M.N. Freitas, J.M. Marchetti, Nimesulide PLA microspheres as a potential sustained release system for the treatment of inflammatory diseases, Int. J. Pharm. 295 (1–2) (2005) 201–211, https://doi.org/10.1016/j.ijpharm.2005.03.003.

[14] Y.P. Guo, T. Long, Z.F. Song, Z.A. Zhu, Hydrothermal fabrication of ZSM-5 zeolites: Biocompatibility, drug delivery property, and bactericidal property, J. Biomed. Mater. Res. - Part B Appl. Biomater. 102 (3) (2014) 583–591, https://doi.org/10.1002/jbm.b.33037.

[15] J. Hao, I. Stavljenić Milašin, Z. Batu Eken, M. Mravak-Stipetic, K. Pavelić, F. Ozer, Effects of zeolite as a drug delivery system on cancer therapy: a systematic review, Molecules 26 (20) (2021) 6196, https://doi.org/10.3390/molecules26206196.

[16] R.E. Harris, J. Beebe-Donk, H. Doss, D.B. Doss, Aspirin, ibuprofen, and other non-steroidal anti-inflammatory drugs in cancer prevention: a critical review of non-selective COX-2 blockade, Oncol. Rep. 13 (4) (2005) 559–583.

[17] Q. He, Y.u. Gao, L. Zhang, Z. Zhang, F. Gao, X. Ji, Y. Li, et al., A pH-responsive mesoporous silica nanoparticles-based multi-drug delivery system for overcoming multi-drug resistance, Biomaterials 32 (30) (2011) 7711–7720.

[18] T. Higuchi, Rate of release of medicaments from ointment bases containing drugs in suspension, J. Pharm. Sci. 50 (10) (1961) 874–875, https://doi.org/10.1002/jps.2600501018.

[19] A.W. Hixson, J.H. Crowell, Dependence of reaction velocity upon surface and agitation, Ind. Eng. Chem. 23 (8) (1931) 923–931, https://doi.org/10.1021/ie50260a018.

[20] S. Honary, F. Zahir, Effect of zeta potential on the properties of nano-drug delivery systems - a review (Part 1), Trop. J. Pharm. Res. 12 (2) (2013) 255–264, https://doi.org/10.4314/tjpr.v12i2.19.

[21] S. Iqbal Farooqi, N. Arshad, F. Perveen, P. Ali Channar, A. Saeed, A. Javed, T. Hökelek, U. Flörke, Structure and surface analysis of ibuprofen-organotin conjugate: potential anti-cancer drug candidacy of the compound is proven by in-vitro DNA binding and cytotoxicity studies, Polyhedron 192 (2020) 114845, https://doi.org/10.1016/j.poly.2020.114845.

[22] V. Karavelidis, E. Karavas, D. Giliopoulos, S. Papadimitriou, D. Bikiaris, Evaluating the effects of crystallinity in new biocompatible polyester nanocarriers on drug release behavior, Int. J. Nanomed. 6 (2011) 3021–3032, https://doi.org/10.2147/ijn.s26016.

[23] M. Khatamian, B. Divband, F. Farahmand-Zahed, Synthesis and characterization of Zinc (II)-loaded Zeolite/Graphene oxide nanocomposite as a new drug carrier, Mater. Sci. Eng., C 66 (2016) 251–258, https://doi.org/10.1016/j.msec.2016.04.090.

[24] R.W. Korsmeyer, R. Gurny, E. Doelker, P. Buri, N.A. Peppas, Mechanisms of solute release from porous hydrophilic polymers, Int. J. Pharm. 15 (1) (1983) 25–35, https://doi.org/10.1016/0378-5173(83)90064-9.

[25] D. Krajišnik, A. Daković, A. Malenović, M. Kragović, J. Milić, Ibuprofen sorption and release by modified natural zeolites as prospective drug carriers, Clay Miner. 50 (1) (2015) 11–22, https://doi.org/10.1180/claymin.2015.050.1.02.

[26] H. Lokhandwala, A. Deshpande, S. Deshpande, Kinetic modeling and dissolution profiles comparison: an overview, Int. J. Pharm. Bio. Sci 4 (1) (2013) 728–773.

[27] S. Mallick, S. Pattnaik, K. Swain, P.K. De, A. Saha, G. Ghoshal, A. Mondal, Formation of physically stable amorphous phase of ibuprofen by solid state milling with kaolin, Eur. J. Pharm. Biopharm. 68 (2) (2008) 346–351, https://doi.org/10.1016/j.ejpb.2007.06.003.

[28] I.M. Minisy, N.A. Salahuddin, M.M. Ayad, In vitro release study of ketoprofen - loaded chitosan / polyaniline nanofibers, Polym. Bull. 78 (10) (2021) 5609–5622, https://doi.org/10.1007/s00289-020-03385-z.

[29] R. Mujoriya, R.B. Bodla, K. Dhamande, D. Singh, L. Patle, Niosomal drug delivery system: The magic bullet, J. Appl. Pharm. Sci. 1 (9) (2011) 20–23.

[30] Y.A.B. Neolaka, H. Darmokoesoemo, A.A. Adu, Y. Lawa, J. Naat, A.A.P. Riwu, M. F. Bui, E.C. Wila, M.A. Fahirah, T.A. Budiastant, B.A. Widyaningrum, M. Riwu, H. S. Kusuma, Study of mordenite natural zeolite type modified by Cu(II) cation as an oral safe drug carrier for ibuprofen and meloxicam, J. Mol. Liq. 352 (2022) 118734.

[31] Y.A.B. Neolaka, E.B.S. Kalla, G. Supriyanto, N.N.T. Puspaningsih, Adsorption of hexavalent chromium from aqueous solutions using acid activated of natural zeolite collected from Ende-Flores, Indonesia, Rasāyan J. Chem. 10 (2) (2017) 606–612.

[32] Y.A.B. Neolaka, Y. Lawa, J. Naat, A.A.P. Riwu, Y.E. Lindu, H. Darmokoesoemo, B. A. Widyaningrum, M. Iqbal, H.S. Kusuma, Evaluation of magnetic material IIP@ GO-Fe3O4 based on Kesambi wood (Schleichera oleosa) as a potential adsorbent for the removal of Cr(VI) from aqueous solutions, React. Funct. Polym. 166 (2021) 105000.

[33] M.P. Paarakh, P.A.N.I. Jose, C.M. Setty, G.V. Peter, Release Kinetics – Concepts and Applications, Int. J. Pharm. Res. Technol. 8 (1) (2019) 12–20, https://doi.org/10.31838/ijprt/08.01.02.

[34] N.F. Paretsis, V.G. Junior, N.G.T. de Q. Hazarbassanov, G.M. Marcondes, A.M.de G. Plepis, V.da C.A. Martins, A.L. do V. De Zoppa, In vitro evaluation of hydroxyapatite, chitosan, and carbon nanotube composite biomaterial to support bone healing, Braz. J. Vet. Res. Anim. Sci. 58 (2021) e179885, https://doi.org/10.11606/issn.1678-4456.bjvras.2021.179885.

[35] L.D. Pedro-Hernández, E. Martínez-Klimova, S. Cortez-Maya, S. Mendoza-Cardozo, T. Ramírez-Ápan, M. Martínez-García, Synthesis, characterization, and nanomedical applications of conjugates between resorcinarene-dendrimers and

ibuprofen, Nanomaterials 7 (7) (2017) 163, https://doi.org/10.3390/nano7070163.
[36] N.A. Peppas, J.J. Sahlin, A simple equation for the description of solute release. III. Coupling of diffusion and relaxation, Int. J. Pharm. 57 (2) (1989) 169–172, https://doi.org/10.1016/0378-5173(89)90306-2.
[37] K.H. Ramteke, P.A. Dighe, A.R. Kharat, S.V. Patil, Mathematical models of drug dissolution: a review, Sch. Acad. J. Pharm 3 (5) (2014) 388–396.
[38] H. Raslan, H. Maswadeh, In vitro dissolution kinetic study of theophylline from mixed controlled release matrix tablets containing hydroxypropylmethyl cellulose and glycerylbehenate, Indian J. Pharm. Sci. 68 (3) (2006) 308–312, https://doi.org/10.4103/0250-474x.26658.
[39] J. Saha, J. Podder, Crystallization of zinc sulphate single crystals and its structural, thermal and optical characterization, J. Bangladesh Acad. Sci. 35 (2) (2011) 203–210, https://doi.org/10.3329/jbas.v35i2.9426.
[40] N. Salahuddin, S. Awad, Optimization delivery of 5 - fluorouracil onto different morphologies of ZnO NPs: release and functional effects against colorectal cancer cell lines, Chem. Papers (2021), https://doi.org/10.1007/s11696-021-01625-8.
[41] N. Salahuddin, E. Ibrahim, M. El-kemary, Surfactant free-poly (lactic-co-glycolic acid) coated artesunate loaded citrate-functionalized hydroxyapatite nanorods as a nanocapsule for improving artesunate delivery and antitumor efficiency, Ceram. Int. 48 (10) (2022) 13452–13463, https://doi.org/10.1016/j.ceramint.2022.01.223.
[42] N. Sizochenko, A. Mikolajczyk, M. Syzochenko, T. Puzyn, J. Leszczynski, Zeta potentials (ζ) of metal oxide nanoparticles: A meta-analysis of experimental data and a predictive neural networks modeling, NanoImpact 22 (2021), 100317, https://doi.org/10.1016/j.impact.2021.100317.
[43] C.-Y. Sun, C. Qin, X.-L. Wang, G.-S. Yang, K.-Z. Shao, Y.-Q. Lan, E.-B. Wang, Zeolitic imidazolate framework-8 as efficient pH-sensitive drug delivery vehicle, Dalton Trans. 41 (23) (2012) 6906–6909, https://doi.org/10.1039/C2DT30357D.
[44] W. Sun, H. Li, H. Li, S. Li, X. Cao, Adsorption mechanisms of ibuprofen and naproxen to UiO-66 and UiO-66-NH2: Batch experiment and DFT calculation, Chem. Eng. J. 360 (2019) 645–653, https://doi.org/10.1016/j.cej.2018.12.021.
[45] J.M. Unagolla, A.C. Jayasuriya, Drug transport mechanisms and in vitro release kinetics of vancomycin encapsulated chitosan-alginate polyelectrolyte microparticles as a controlled drug delivery system, Eur. J. Pharm. Sci. 114 (September 2017) (2018) 199–209, https://doi.org/10.1016/j.ejps.2017.12.012.
[46] N. Vilaça, R. Amorim, A.F. Machado, P. Parpot, M.F.R. Pereira, M. Sardo, F. Baltazar, Potentiation of 5-fluorouracil encapsulated in zeolites as drug delivery systems for in vitro models of colorectal carcinoma, Colloids Surf., B 112 (2013) 237–244, https://doi.org/10.1016/j.colsurfb.2013.07.042.
[47] Z. Wang, B. Chen, G. Quan, F. Li, Q. Wu, L. Dian, C. Wu, Increasing the oral bioavailability of poorly water-soluble carbamazepine using immediate-release pellets supported on SBA-15 mesoporous silica, Int. J. Nanomed. 7 (2012) 5807–5818, https://doi.org/10.2147/IJN.S37650.
[48] Y. Zhang, X. Xu, W.-S. Xu, Influence of Ionic Interaction Strength on Glass Formation of an Ion-Containing Polymer Melt, Macromolecules 54 (20) (2021) 9587–9601, https://doi.org/10.1021/acs.macromol.1c01719.